Separation and Purification Technology 333 (2024) 125903

Contents lists available at ScienceDirect

Separation and Purification Technology

journal homepage: www.elsevier.com/locate/seppur

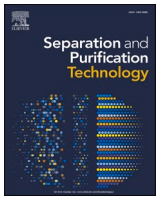

Separation of cationic methylene blue dye from its aqueous solution by S-sulfonated wool keratin-based sustainable electrospun nanofibrous membrane biosorbent

Md. Nahid Pervez [a], Mohammad Mahbubul Hassan [b,c,*], Vincenzo Naddeo [a,*]

[a] Sanitary Environmental Engineering Division (SEED), Department of Civil Engineering, University of Salerno, via Giovanni Paolo II 132, 84084 Fisciano, SA, Italy
[b] Bioproduct and Fiber Technology Team, AgResearch Limited, 1365 Springs Road, Lincoln, Christchurch 7674, New Zealand
[c] Fashion, Textiles and Technology Institute, University of the Arts London, 105 Carpenter's Road, Stratford, London E20 2AR, United Kingdom

ARTICLE INFO

Keywords:
Dye separation
S-sulfonated keratin nanofibrous membrane
Adsorption
Cationic dye
Adsorption kinetics
Adsorption isotherm

ABSTRACT

The use of electrospun nanofibrous membranes for the treatment of dyehouse effluent is drawing attention because of their high surface area, and dye adsorption capability. In this work, nanofibrous membranes of S-sulfonated wool keratin protein/poly(vinyl alcohol) or PVA were prepared by electrospinning, and their effectiveness as an adsorbent for the removal of cationic methylene blue (MB) dye was studied. The electrospun nanofibers fabricated from keratin/PVA had a considerably finer average diameter (79.0 nm) compared to the average diameter (255.4 nm) exhibited by nanofibers produced from PVA alone. The optimal adsorption capacity was attained at a pH value close to neutral at ambient temperature (238.7 mg g^{-1}), and the pseudo-second-order model was determined to be a reliable fit for the experimental data. Based on the fitted Langmuir model and MB adsorption data, the adsorption mechanism followed a monolayer pattern on the surface of the membrane. The MB dye adsorption capacity was slightly influenced by the presence of sodium chloride. The study demonstrated that the PVA/keratin nanofibrous membrane exhibited good reusability as only a small loss in absorption capacity was observed after three recycling and reuses. The developed biosorbent could be suitable for the high removal of dyes from textile dyehouse effluent.

1. Introduction

Textile dyehouse effluent is one of the major chemical industry pollutants and has received significant attention due to its evidenced toxicity to aquatic species and human beings [1,2]. Cationic dyes are extensively used in several industrial sectors like textiles, leather, pharmaceuticals, and aquaculture, and have high detrimental environmental impacts. They are highly popular for the dyeing of acrylic, cationic dyeable polyester, and jute fibers as they can produce bright shades, but they are relatively toxic compared to other textile dyes [3]. Of the cationic basic dyes, methylene blue (MB) dye is frequently used in textile dyeing with evidence of high toxicity and therefore it is crucial to undertake appropriate measures to limit its release into the surrounding ecosystem [4,5]. Numerous studies were carried out based on various approaches, such as catalysis, filtration, membrane technology, biological processes, ozonation, and adsorption for the elimination of dyes from dyehouse effluent [6–8]. Among them, adsorption methods are highly popular because of their versatility, low cost, the possibility of recovery of pollutants intact, and recycling and reuse of the used adsorbents. Bio-based adsorbents have been extensively studied for the removal of cationic dyes from effluent [9,10]. Nanofibrous membrane-based adsorbents for removing dyes from wastewater have been identified as an effective technology due to their high surface area, high effectiveness, and minimal environmental impact [11,12].

Recently, there has been a growing interest in utilizing electrospun nanofibrous membranes as an adsorbent for the removal of dyes from dyehouse effluent due to their many beneficial characteristics, such as a high degree of porosity characterized by interconnected pores, a substantial surface area-to-volume ratio, and the ability to tailor surface functional properties for the removal of specific pollutants [13]. The process of nanofiber formation by electrospinning is an electrohydrodynamic process, in which a liquid droplet is electrified to

* Corresponding authors at: Fashion, Textiles and Technology Institute, University of the Arts London, 105 Carpenter's Road, Stratford, London E20 2AR, United Kingdom (M.M. Hassan).
E-mail addresses: mahbubul.hassan@arts.ac.uk (M.M. Hassan), vnaddeo@unisa.it (V. Naddeo).

https://doi.org/10.1016/j.seppur.2023.125903
Received 9 October 2023; Received in revised form 13 November 2023; Accepted 28 November 2023
Available online 2 December 2023

generate a jet followed by stretching and elongation to generate fiber [14]. The fundamental components of an electrospinning setup consist of a high-voltage power supply, a spinneret or hypodermic needle with a blunt tip, a conductive but grounded collector or receiving object on which the formed nanofiber can deposit, and a syringe pump. In electrospinning, the viscous liquid is extruded from the needle tip to produce a pendant droplet due to surface tension. Upon electrification, the electrostatic repulsion among the surface charges due to the disparity in electrical potential between the spinneret tip and the grounded collector deforms the droplet into a Taylor cone. From it, a charged jet of solution is ejected, which initially extends in a straight line and then undergoes strong turbulent motions because of bending instabilities. As the jet is stretched into finer diameters, the containing solvent quickly evaporates forming solid fibers and they deposit on the grounded collector. Any conductive materials, such as copper, aluminum, and stainless steel can work as a grounded collector to collect the formed nanofibrous membrane [15,16].

To date, a range of natural polymers has been utilized to produce electrospun nanofibrous membrane-based adsorbents that demonstrated a high dye removal efficacy from dyehouse effluent [17,18]. Natural polymers are usually mixed with another high molecular weight synthetic polymer as a carrier to improve their electrospinnability. The natural polymers studied are chitosan mixed with polyvinyl alcohol [18], cellulose acetate mixed with polyaniline/β-cyclodextrin [19], zein protein mixed with polyamide [20], and silk fibroin mixed with polyacrylonitrile [21]. Nanofibrous membrane adsorbent made from a mixed solution of silk fibroin and polyacrylonitrile 7.5 % polyaniline and titanium dioxide removed ~ 92 % of a reactive black dye [21]. The Chitosan/PVA composite nanofibrous membrane showed quite poor methylene blue dye binding capacity, only 75.8 mg g^{-1} [18]. Proteins are not commonly used alone to produce electrospun nanofibrous membranes due to their poor electrospinnability, although they have excellent biocompatibility and biodegradability. Keratin, a prominent protein found in various natural materials such as wool, hair, nails, horn, feathers, beaks, claws, and hooves of animals and birds, is a polyamino acid having a high number of anionic carboxyl groups that can be utilized for binding cationic dyes [22,23]. Keratin is an abundantly available biopolymer as animal slaughterhouses and the wool industry produces millions of tons of keratin containing biomass every year. Due to the aforementioned factors, keratin presents itself as a compelling and economically viable biomass resource for exploitation. Regrettably, the conversion of keratin into a nanofibrous membrane through the process of electrospinning poses significant challenges due to its low molecular weight and brittleness [24]. Hence, combining keratin protein with compatible water-soluble polymers with high molecular weight would be a viable method for fabricating electrospun keratin nanofibrous membranes. Polyvinyl alcohol (PVA) is a synthetic polymer with a range of advantageous characteristics, such as favorable biocompatibility, notable water solubility, and exceptional chemical and thermal stability [25]. Considerable emphasis has been placed on the investigation of PVA-based nanofibrous membranes as a promising catalyst carrier for wastewater treatment owing to ample hydroxyl groups within their side chains [26,27]. PVA has high compatibility with wool keratin with tailored molecular weight and therefore could be an ideal polymer to add to keratin to produce keratin nanofibrous membrane. Karim et al. demonstrated that nanofibrous membranes composed of poly(vinyl alcohol) and chitosan exhibited high Pb(II) and Cd(II) binding capacity, 266.0 and 148.0 mg g^{-1} respectively [28]. In recent years, there has been a significant increase in the fabrication and utilization of electrospun nanofibrous membranes composed of keratin in combination with PVA for biomedical applications [29,30]. Nevertheless, there is currently a lack of research on the application of PVA/keratin composite electrospun nanofibrous membranes in the field of wastewater treatment, indicating the need for additional exploration in this area.

Electrospun nanofibrous membrane adsorbents extracted from wool fiber and feathers have been studied for the removal of heavy metal ions and dyes from their aqueous solutions in batches as well as under dynamic conditions. For example, Aluigi et al. reported the extraction of hydrolyzed keratin from wool fiber by sulfitolysis and electrospun nanofibrous membrane of 223 ± 74 nm diameter nanofibers was produced from 15 % solution of hydrolyzed keratin by electrospinning, which showed quite low MB dye binding capacity [31]. However, no published literature reported the removal of cationic dye by nanofibrous membranes made from S-sulfonated keratin/PVA blends, which may show better cationic dye binding capacity compared to the normal keratin-based nanofibrous membranes.

Usually, wool fibers available underneath the belly of sheep are not used in textile manufacturing and they are discarded as waste. In this work, S-sulfonated keratin intermediate filament protein was extracted from waste merino wool fibers by sulfitolysis followed by oxidation, which formed S-sulfonated keratin containing more anionic Bunte salt groups compared to keratin extracted by sulfitolysis alone considerably increasing the cationic MB dye-binding sites. The electrospinning of a 50/50 mixture of S-sulfonated keratin and PVA produced nanofibers of ultrathin diameters, which provided excellent MB dye binding capacity. The subsequent investigation focused on systematically analyzing the nanofibrous membrane's capability for dye adsorption, altering several operational parameters, including pH, contact time, initial concentration of MB dye, and ionic strength. Additionally, a reusability test of the adsorbent material was carried out to find its suitability for practical application.

2. Experimental

2.1. Materials and reagents

The high molecular weight S-sulfonated keratin protein used in this work was extracted from waste New Zealand merino wool fibers by oxidative sulfitolysis, which was supplied by Keraplast Limited (New Zealand). Poly(vinyl alcohol) (PVA) with an average molecular weight of 89,000 ($M_n = 89000$) and 99 % hydrolyzed was procured from Sigma-Aldrich Chemicals (USA). The methylene blue (purity ≥ 82 %) was acquired from Sigma Aldrich Co., Ltd. (Darmstadt, Germany). All other chemicals and reagents were used directly in the current study without any modifications.

2.2. Electrospinning of PVA/keratin nanofibrous membrane

The fabrication process of the nanofibrous membrane is presented by a schematic diagram in Fig. 1. To prepare the keratin/PVA mixed solution, 4 g PVA was dissolved in 98 mL water by heating at 90 °C, and the evaporated water was replenished with the addition of fresh water. Then 4 g keratin and 0.8 g glycerol were added to it to make a 50/50 (wt/wt) mixture of keratin and PVA solution. The added keratin solution was then dissolved by adding 2 mL of concentrated alkali solution drop-by-drop so that the pH of the solution did not go over 9.0. The viscous solution was loaded in a 10-mL size Terumo syringe, which was placed in a KDS syringe pump (Model 100, KDS Scientific, USA) to control the fluid flow fed to the spinneret. The electrospinning was carried out using an Electrospinz electrospinning machine (Electrospinz Limited, Blenheim, New Zealand) using 20 kV power and 1 mL h^{-1} flow rate. A rotating stainless-steel disk of 5.5 cm diameter was used as a grounded collector. Electrospinning was performed at room temperature (20 °C) and 45 % relative humidity by maintaining a fixed needle-to-collector distance of 20 cm. The mentioned conditions were found to be the best to produce bead-free uniform-sized nanofibers.

2.3. Characterization

A field emission scanning electron microscope (FE-SEM, FEI Nova NanoSEM450, Thermo Fisher Scientific Inc., Waltham, MA, USA) was used to study the morphology of the nanofibrous membrane. A section of

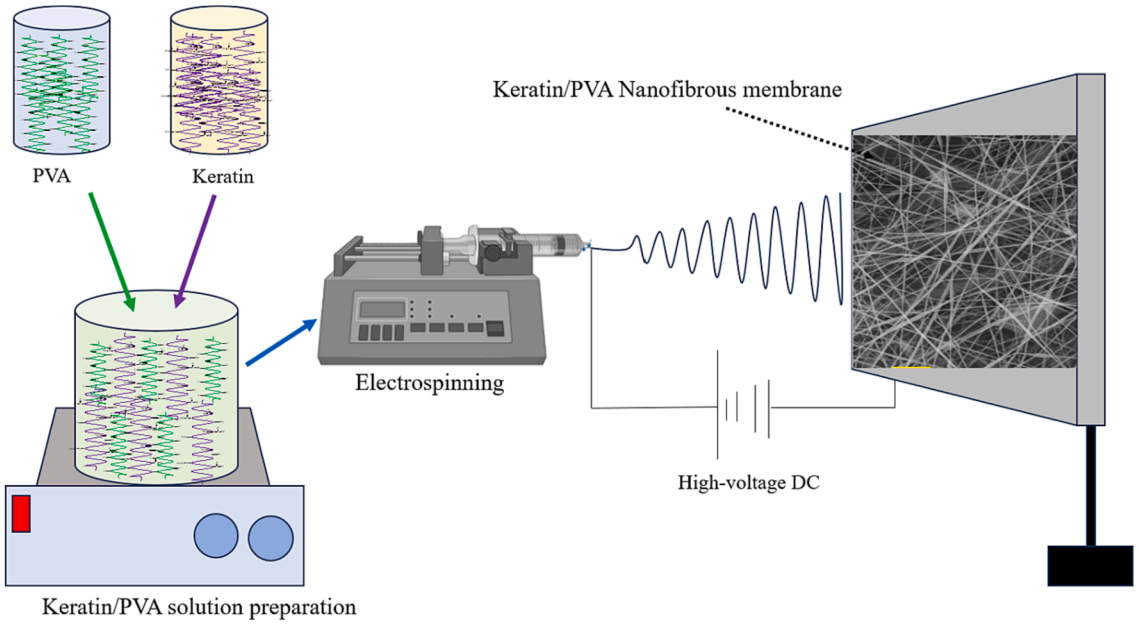

Fig. 1. Schematic diagram of fabrication of keratin/PVA nanofibrous membrane by electro-spinning.

membranes was placed on a conductive glued tape placed on an aluminum stub and then loaded in the SEM. The images were acquired using an incident electron beam energy at 15 kV. The acquired SEM images were utilized to analyze the diameter distribution behavior of the membrane, which was processed using ImageJ software (https://imagej.nih.gov/ij/download.html, accessed on 30 August 2023). The porosity of PVA and keratin/PVA nanofibrous membranes was measured using the liquid displacement method at 20 ± 2 °C [32]. The porosity of the membranes was calculated according to Eq. (1).

$$Porosity(\%) = [\frac{W_2 - W_1}{\rho Vs}] \times 100 \quad (1)$$

where W_1 and W_2 are weights of the nanofibrous membrane before and after immersion in distilled water for 24 h respectively, ρ is the density of water and Vs is the volume of the nanofibrous membrane [33]. The tensile properties of the PVA and keratin/PVA nanofibrous membrane were measured by using an Instron universal tensile testing machine (Model: 4204, Instron Corporation, Norwood, USA). The tensile properties were measured according to the ASTM standard D638A using a strain rate of 10 mm min^{-1} and a sample size of 75 mm × 10 mm. Ten replications of each formulation were conducted, and average values are reported here. The attenuated total reflectance-Fourier transform infrared (ATR-FTIR) spectra of neat PVA and 50/50 keratin/PVA nanofibrous membranes were acquired with a Nicolet FTIR spectrophotometer (Model: SummitPro, ThermoFisher Scientific Corporation, USA) using a diamond crystal. 128 scans with a resolution of 2 cm^{-1} were performed for each spectrum to achieve optimal signal-to-noise ratio and the averages are shown.

2.4. Batch adsorption studies

The batch adsorption experiments were conducted at room temperature using the VWR polypropylene centrifuge tubes. Briefly, a volume of 50 mL of a solution containing 200 mg L^{-1} of MB dye was introduced into each tube. Subsequently, 5 mg of adsorbents were added to the tubes. The mixture was then subjected to magnetic agitation under neutral pH conditions. In each experimental trial, a certain volume of the solution was systematically extracted at regular time intervals and afterward subjected to filtration using a 0.45 μm membrane filter. The concentration of MB dye was measured at a specific wavelength of 664 nm using a Perkin-Elmer UV–Vis spectrophotometer (Model: Lambda 25, Perkin Elmer Corporation, Waltham, USA). The adsorption capacity of MB dye by PVA and keratin/PVA nanofibrous membranes was calculated using the Eq. (2) shown below:

$$Q_e = \frac{V \times (C_0 - C_e)}{m} \quad (2)$$

The variable Q_e (mg g^{-1}) represents the equilibrium adsorption quantities, C_e (mg L^{-1}) represents the equilibrium concentration, C_0 (mg L^{-1}) represents the starting concentration of MB dye, m (g) represents the quantity of adsorbent used, and V (L) represents the volume of the solution being adsorbed.

2.4.1. Adsorption kinetics and isotherms

At pH 7, 50 mL of MB dye solution (200 mg L^{-1}) and 5 mg of adsorbent were placed in separate test tubes to conduct batch adsorption kinetic measurements. The kinetics performance was investigated by measuring the sample's adsorption capacity at a predetermined contact time. Adsorption isotherms were also studied by introducing a fixed amount of adsorbent (5 mg) to 50 mL solutions ranging from 50 to 400 mg L^{-1} MB dye in a series of tubes. The final concentration at equilibrium was determined by filtering the solution and measuring the absorbance of the MB dye solution.

2.4.2. Effect of pH

5 mg of the as-prepared nanofibrous membranes were added to the MB dye solution (50 mL, dye concentration: 200 mg L^{-1}) at various initial pHs to test the influence of pH on the developed keratin/PVA nanofibrous membrane's MB dye removal and dye adsorption capacity. The pH of the MB dye solutions was set from 2 to 10 and the adsorption was conducted for 12 h.

2.4.3. Effect of ionic strength

The impact of ionic strength on the adsorbability of MB dye was assessed using the usual adsorption method in the presence of the developed nanofibrous membranes. Using a similar methodology, a quantity of 5 mg of adsorbents was added to an MB dye solution in a centrifuge tube containing 50 mL of 200 mg L^{-1} MB dye at pH 7. The effect of ionic strength on the MB dye absorption capacity of nanofibrous membranes was carried out by adding different concentrations of NaCl (ranging from 0.1 M to 0.5 M) to the dye solution and by carrying out the

absorption test for 12 h at room temperature.

2.4.4. Reusability

The regeneration of the adsorbents was carried out by immersing them in a 2 mM hydrochloric acid (HCl) solution for 6 h at room temperature releasing the absorbed dye. Three regeneration cycles were conducted using the same experimental conditions, whereby each examined adsorbent was subjected to two washes with deionized water before being prepared for the subsequent adsorption cycle. Subsequently, the quantification of MB dye was conducted to determine the adsorption capability.

3. Results and discussion

3.1. Characterization of keratin nanomembrane adsorbent

The surface morphologies of neat PVA and keratin/PVA composite membranes were analyzed using SEM. Fig. 2a illustrates a representative SEM micrograph of a pristine PVA nanofibrous membrane. The micrograph shows the produced PVA nanofibers are quite uniformly sized with an average diameter of ~ 225 nm (Fig. 2c). The formed nanofibers are quite randomly oriented across the membrane, exhibiting a uniform distribution without any noticeable bead formation. The nanofibers produced from a mixed solution of keratin and PVA produced smooth surfaces as shown in Fig. 2b, and the produced nanofibers possess an exceptionally small diameter of ~ 79 nm (Fig. 2d). The replacement of 50 % of high molecular weight PVA used in this work with lower molecular weight keratin considerably reduced the viscosity of the keratin/PVA solution and electrospinning of that solution produced nanofibers of finer diameter compared to the nanofibers produced from neat PVA solution of the same weight%. Several researchers also reported that the viscosity of the polymer solution affects the diameter of nanofibers produced by electrospinning and an increase in the viscosity increases the diameter of the nanofibers [34,35]. The morphological structure of nanofibers produced from a keratin/PVA mixed solution exhibited no noticeable phase separation between keratin and PVA during the electrospinning process, suggesting excellent compatibility between the two polymer phases.

The pore size and porosity of the produced nanofibrous membranes of PVA and keratin PVA are presented in Table S1 (Supplementary Materials). The nanofibrous membrane made from neat PVA shows a larger pore size and higher porosity compared to the nanofibrous membrane made from a mixture of keratin and PVA.

The mechanical properties of PVA and keratin/PVA nanofibrous membranes are also presented in Table S1 (Supplementary Materials). The nanofibrous membrane made from neat PVA exhibited tensile strength and elongation at break of 16.7 ± 1.1 MPa and 27.0 ± 3.0 % respectively. The addition of keratin to PVA decreased the tensile strength of the composite nanofibrous membrane to 14.3 ± 1.5 MPa. The keratin and PVA formed hydrogen bonding in the composite nanofibrous membrane, which reduced its elongation at the break.

FTIR spectral analysis was carried out to determine the interaction between PVA and keratin in the electrospun composite nanofibrous membrane. Fig. S1 (Supplementary Materials) shows the FTIR spectrum

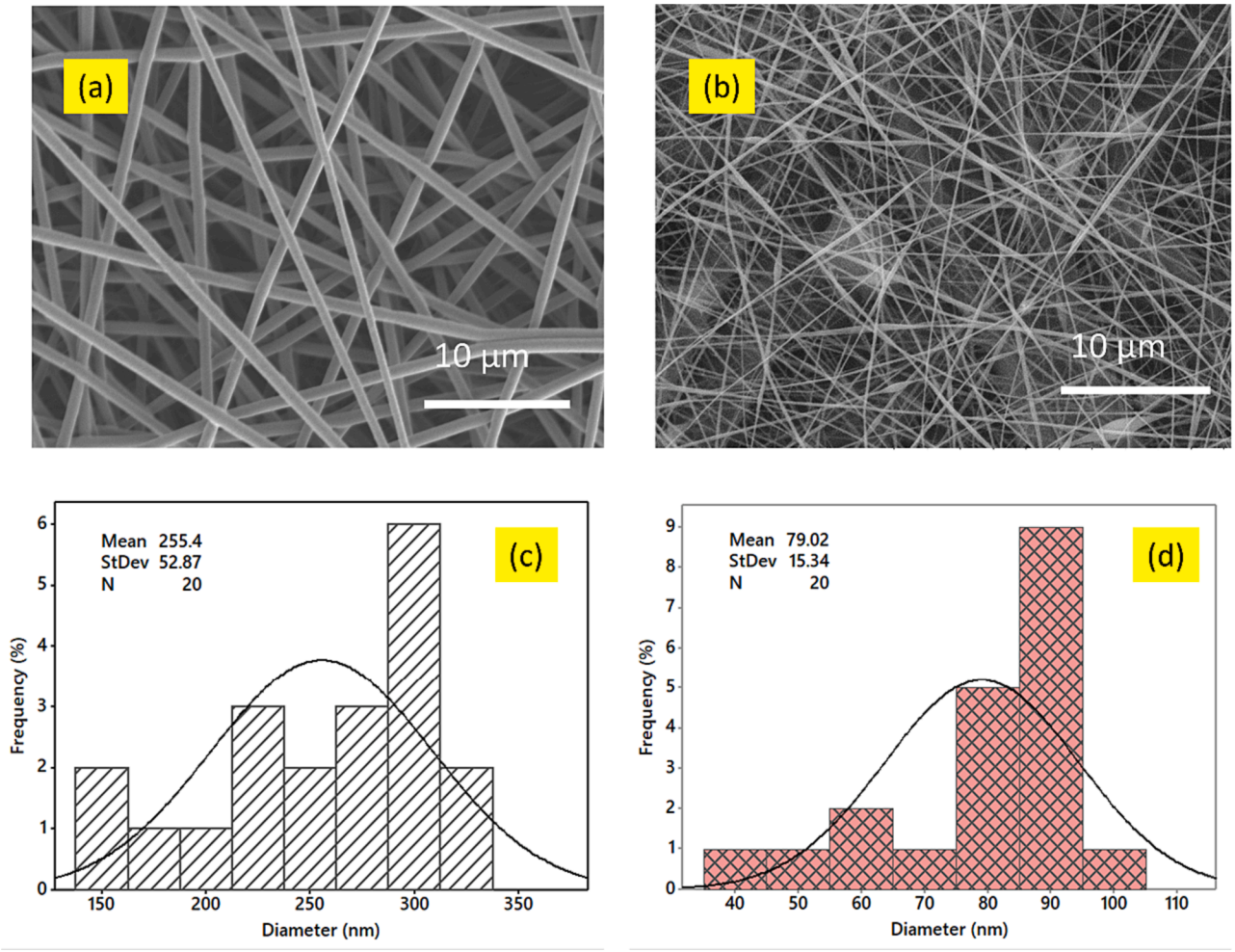

Fig. 2. SEM images and diameter distribution of (a, c) PVA and (b, d) keratin-PVA nanofibrous membrane.

of the pure PVA nanofibrous membrane. The IR absorption band observed at 3342 cm^{-1} is attributed to the stretching vibration of the –OH groups of PVA. Similarly, the IR bands observed at 2923 and 2877 cm^{-1} are associated with the asymmetric and symmetric stretching vibration of the $–CH_2$ groups of PVA respectively. The absorption band observed at 1650 cm^{-1} is associated with the stretching vibration absorption of the –OH groups due to the absorption of moisture by the PVA [36]. The appearance of the IR bands at 1421 and 1379 cm^{-1} may be attributed to the bending of the CH_3 and CH_2 groups respectively. Similarly, the IR band detected at 879 cm^{-1} can be ascribed to the rocking vibrations of the CH_2 group [37]. Furthermore, the band observed at 1087 cm^{-1} is indicative of the stretching of the C–O bond.

After the addition of keratin to the PVA spinning solution, the spectra of the resulting composite nanofibers displayed IR absorption bands at 1650, 1540, and 1248 cm^{-1} corresponding to the amide I (C = O stretching vibration), amide II (N–H bending) and amide III (C–H stretching vibration) regions of wool keratin protein [38]. The new IR band at 1022 cm^{-1} is associated with the stretching vibrations of Bunte salt groups of wool keratin protein [39]. The ATR-FTIR spectral analysis suggests the presence of S-sulfonated keratin protein in the keratin/PVA nanofibers. The study revealed that the wavenumbers associated with the distinctive absorption band of hydroxyl groups experienced a downward shift to 3275 cm^{-1} in the keratin/PVA composite nanofibers suggesting hydrogen bond formation between hydroxyl groups of PVA and carboxyl/amino groups of keratin protein [30], which enhanced the electrospinnability of keratin/PVA composite nanofibers.

3.2. Adsorption studies

To identify the dye adsorption performance of neat PVA and keratin/PVA nanofibrous membranes and the optimum dye adsorption conditions, the effect of several process parameters was studied. These included the impact of pH, initial dye concentration, and contact time on MB dye adsorption by the developed adsorbent. Following this, the effect of ionic strength on MB dye adsorption capacity was thoroughly studied, and the recyclability of the adsorption method was conducted to ensure the viability of the prepared nanofibrous membrane adsorbents for practical use. To learn more about how MB dye adsorbs onto electrospun nanofibrous membrane-based adsorbents, kinetics-isotherm fitting was done using Langmuir and Freundlich models.

3.2.1. Effect of pH

The surface charge of adsorbents and adsorbate, as well as the adsorption performance of the adsorbents, may be significantly influenced by the dye solution pH [40]. Hence, an investigation was conducted to determine the adsorption capability of MB dye by PVA and keratin/PVA nanofibrous membranes across different pH ranges (2 to 10). The effect of pH on the MB dye removal and dye binding capacity of the neat PVA and keratin/PVA nanofibrous membranes are shown in Fig. 3. Both nanofibrous membranes showed the poorest dye removal and dye binding capacity at pH 2, which slowly increased with an increase in pH. In the case of the PVA nanofibrous membrane, the maximum MB dye removal and dye binding capacity (48.0 mg g^{-1}) were achieved at pH 7, and no further increase in adsorption was achieved with an increase in pH. At acidic conditions, some level of dye removal was achieved due to hydrophobic-hydrophobic interaction between alkyl groups of dye and methyl groups of PVA (few methyl acetate groups still remained as the PVA used was 99 % hydrolyzed). With an increase in pH at neutral to alkaline conditions, due to deprotonation, the hydroxyl groups of PVA became weakly anionic permitting some level of binding of positively charged MB dye molecules by electrostatic attraction. However, no increase in dye removal and dye binding capacity was achieved when the pH of the dye solution was increased from 7 to 10. In alkaline conditions, PVA nanofibers swelled forming a gel and the glutinousness of PVA probably acted as a barrier hindering the contact between MB dye molecules and hydroxyl groups of the PVA, resulting in a decrease in adsorption rate [41]. Therefore, the increase of dye solution pH from 7 to 10 did not increase the dye removal. The keratin/PVA nanofibrous membrane also showed some level of dye removal and dye binding capacity at pH below 4.5 due to hydrophobic-hydrophobic interaction between dye and methyl groups of PVA, but the MB dye removal and dye binding capacity rapidly increased when the pH of the dye solution was increased from 4.5 to 7 as the adsorption capacity reached its highest level (97.0 mg g^{-1}) at pH 7 due to keratin became negatively charged over pH 5. The MB dye removal and dye binding capacity of keratin/PVA nanofibrous membrane biosorbent was almost double compared to the dye binding capacity exhibited by the neat PVA nanofibrous membrane biosorbent. With a further increase in pH, the MB dye binding capacity of keratin/PVA nanofibrous membrane biosorbent decreased. The possible reason could be due to the partial dissolution of keratin in the dye solution (as keratin is soluble in water in alkaline conditions), and some of the applied keratin protein remained in the treated dye solution increasing its dye concentration and reducing the dye removal.

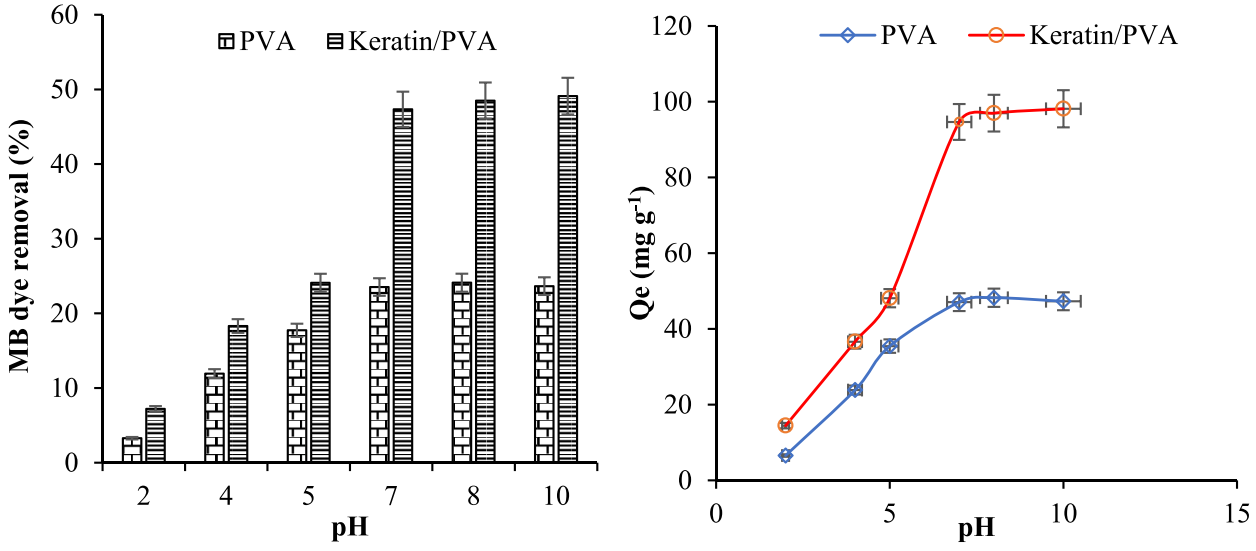

Fig. 3. Effect of pH on MB dye removal (left) and dye adsorption capacity (right).

3.2.2. Effect of initial concentration of MB dye

The initial dye concentration influences the adsorption capacity of dyes since it regulates the availability of binding sites on the adsorbent. Hence, adsorption capacity was measured at a range of initial concentrations of MB dye from 50 to 400 mg L^{-1} while maintaining the pH of the dye solution at 7. The dye removal and dye absorption capacity are shown in Fig. S2 (Supplementary Materials) demonstrating that the initial concentration increase favors the increase in adsorption capacity for both adsorbents. In the case of the PVA/keratin blended nanofibrous membrane, an exponential rise in the dye removal and dye adsorption capacity was seen (ranging from 14.39 to 99.1 mg g^{-1}) when the initial concentration increased from 50 to 200 mg L^{-1}. Subsequently, as the concentration was further increased to 400 mg L^{-1}, a marginal increase in the dye removal and dye adsorption capacity to 101.6 mg g^{-1} was observed. Likewise, a similar pattern was seen in the case of the neat PVA nanofibrous membrane. However, the dye removal and dye adsorption capacity remained significantly low across all concentrations of MB dye, with a maximum capacity of 52.6 mg g^{-1} achieved at a concentration of 400 mg L^{-1}. In both cases, after the concentration exceeds 200 mg L^{-1}, adsorption capacity showed a notable rise until it reached a plateau. The findings of this study suggest that an increase in concentration promotes the process of adsorption by improving mass transfer as the increase in dye concentration increases the availability of dye molecules to bind to the adsorbent, hence serving as the primary driving factor for the adsorption of MB dye.

Furthermore, a significant quantity of MB dye molecules transfers to the nanofibrous membrane's surface from the aqueous phase, increasing dye removal and dye adsorption capacity [42]. The increased concentration of MB dye in the solution increased the availability of more dye molecules to bind to the binding sites of the polymer membrane, hence promoting dye adsorption [43]. Therefore, the increase in the initial concentration of dye solution has a beneficial effect in improving the dye adsorption and binding to the adsorbents.

3.2.3. Adsorption isotherms

Adsorption isotherms play a crucial role in elucidating the dynamics of adsorption phenomena. This investigation examines the connection between the equilibrium concentration of the adsorbent and adsorbate, with a focus on identifying the maximal adsorption capacity. To understand the nature and the mechanism of adsorption, two commonly used non-linear isotherm models, namely the Langmuir and Freundlich models, were tested. The Langmuir fitted model suggests that the adsorption process occurred in a monolayer on a uniform solid adsorbent surface, with no indication of interaction between the adsorbed MB dye molecules and adjacent active sites.

Conversely, the Freundlich fitted isotherm model describes a multilayer adsorption process on a non-uniform solid surface of the adsorbent [44,45]. The fitted curves are shown in Fig. 4, while the derived values for the isotherms are presented in Table 1. The findings indicate that the adsorption isotherm for both membranes followed the Langmuir isotherm model, as shown by the high correlation coefficient values (R^2). This suggests that the adsorption process involves the formation of a monolayer on the heterogeneous surface of the adsorbents. The PVA/keratin nanofibrous membrane had a much higher maximum adsorption capacity of 238.7 mg g^{-1} compared to the neat PVA nanofibrous membrane, which only displayed an adsorption capacity of 94.9 mg g^{-1}. The findings suggest that the PVA/keratin nanofibrous membrane exhibited a notable improvement in the adsorption capacity of MB dye. This improvement may be attributed to the integration of K_L since a higher K_L value of the adsorbent suggests superior adsorption performance at lower concentrations.Table 2..

3.2.4. Adsorption kinetics

Exploration conducted on the kinetics of dye adsorption offers valuable insights into the rate constants associated with the whole adsorption process, specifically concerning the duration of contact between the dye and the adsorbent material [46]. The study examined the kinetics of MB dye adsorption onto nanofibrous membranes composed of PVA and PVA/keratin. The adsorption kinetics of the MB dye adsorption by PVA and keratin/PVA nanofibrous membranes was monitored by measuring the adsorption capacity versus contact time at a fixed initial dye concentration. The dye removal and dye adsorption

Table 1
Adsorption isotherms parameters for MB dye.

Adsorbent	* Langmuir $Q_e = \frac{q_{max} k_L C_e}{1 + k_L C_e}$			* Freundlich $Q_e = K_F C_e^{1/n}$		
	q_{max} (mg g^{-1})	K_L (L mg^{-1})	R^2	K_F (mg g^{-1})	1/n	R^2
PVA	94.8766	0.0030	0.9249	0.8196	0.7022	0.8887
PVA + Keratin	238.6634	0.0023	0.9718	1.3298	0.7592	0.9539

*where q_{max} denotes the maximum adsorption capacity of MB dye (mg g^{-1}); K_L represents the constant of the Langmuir equation, C_e is used for the measurement of solution concentration at equilibrium; 1/n highlights the intensity of the adsorption, and K_F indicates the constant of the Freundlich equation.

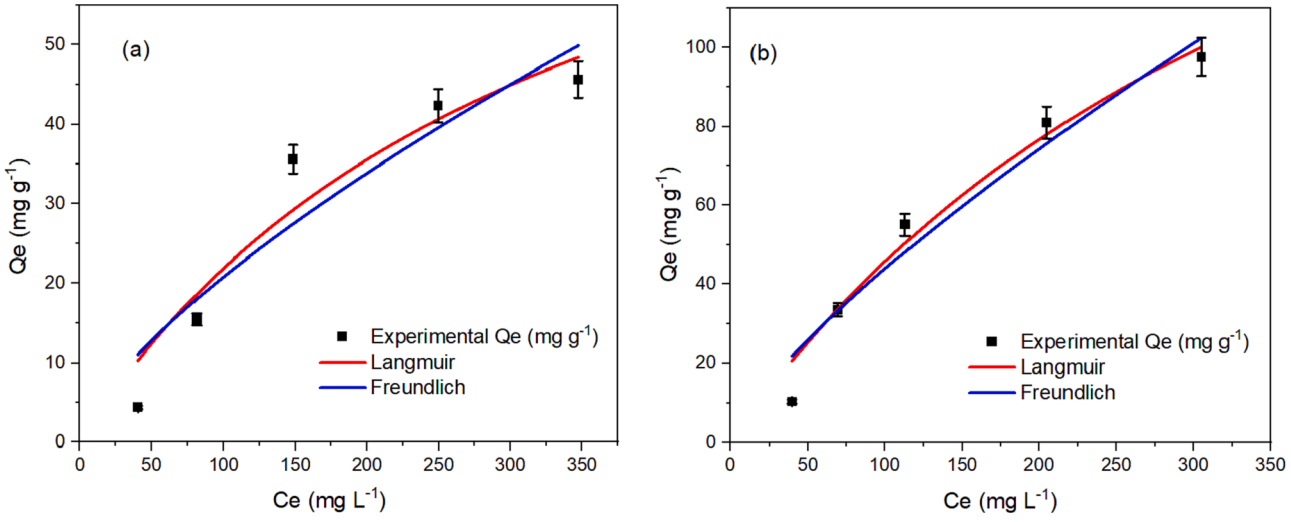

Fig. 4. The adsorption isotherms of MB dye by PVA (a) and PVA/keratin (b) nanofibrous membrane.

Table 2
Kinetics parameters for MB dye adsorption by nanofibrous membranes.

Adsorbent	*Pseudo-first order $Q_t = Q_e(1-e^{-k_1 t})$			*Pseudo-second order $Q_t = \frac{k_2 Q_e^2 t}{1+k_2 Q_e t}$		
	K_1 (min^{-1})	q_e (mg g^{-1})	R^2	K_2 (g mg^{-1} min^{-1})	q_e (mg g^{-1})	R^2
PVA	0.0108	66.3256	0.9020	0.0001	86.1463	0.9302
Keratin + PVA	0.0155	99.0800	0.9847	0.0001	128.8655	0.9876

*where qt (mg g^{-1}) represents the adsorption capacity of MB dye at any time t; k_1 (min^{-1}) and k_2 (g mg^{-1} min^{-1}) are the rate constants for the pseudo-first order and pseudo-second order models respectively.

kinetics for both nanofibrous membrane adsorbents are presented in Fig. 5. The nanofibrous adsorbents initially exhibited a rapid rate of adsorption of MB dye molecules, which then decelerated over time until it reached equilibrium. The equilibrium state of MB dye adsorption on PVA was achieved after 400 min and remained stable for 600 min. In contrast, the PVA/keratin nanofibrous membrane needed 240 min to reach equilibrium, with most of the MB dye molecules being adsorbed during the first 120 min. The findings demonstrate that adding keratin to PVA improved keratin/PVA nanofibrous membrane biosorbent's MB dye adsorption and binding performance, as shown by an increase in adsorption active sites available for capturing MB dye.

Furthermore, the kinetics of adsorption were modeled using nonlinear pseudo-first-order (PFO) and pseudo-second-order (PSO) equations. The fitted curves are shown in Fig. 5(a) and 5(b), while the corresponding estimated fitted values are presented in Table 2. In the case of pure PVA nanofibrous membrane adsorbent, the correlation coefficient exhibited a slightly higher value for PSO (R2 = 0.9302) than PFO (R^2 = 0.9020). In contrast, a lower correlation coefficient was obtained for PFO (R^2 = 0.9847) in comparison to PSO (R^2 = 0.9876) for the PVA/keratin nanofibrous membrane. These findings indicate that the

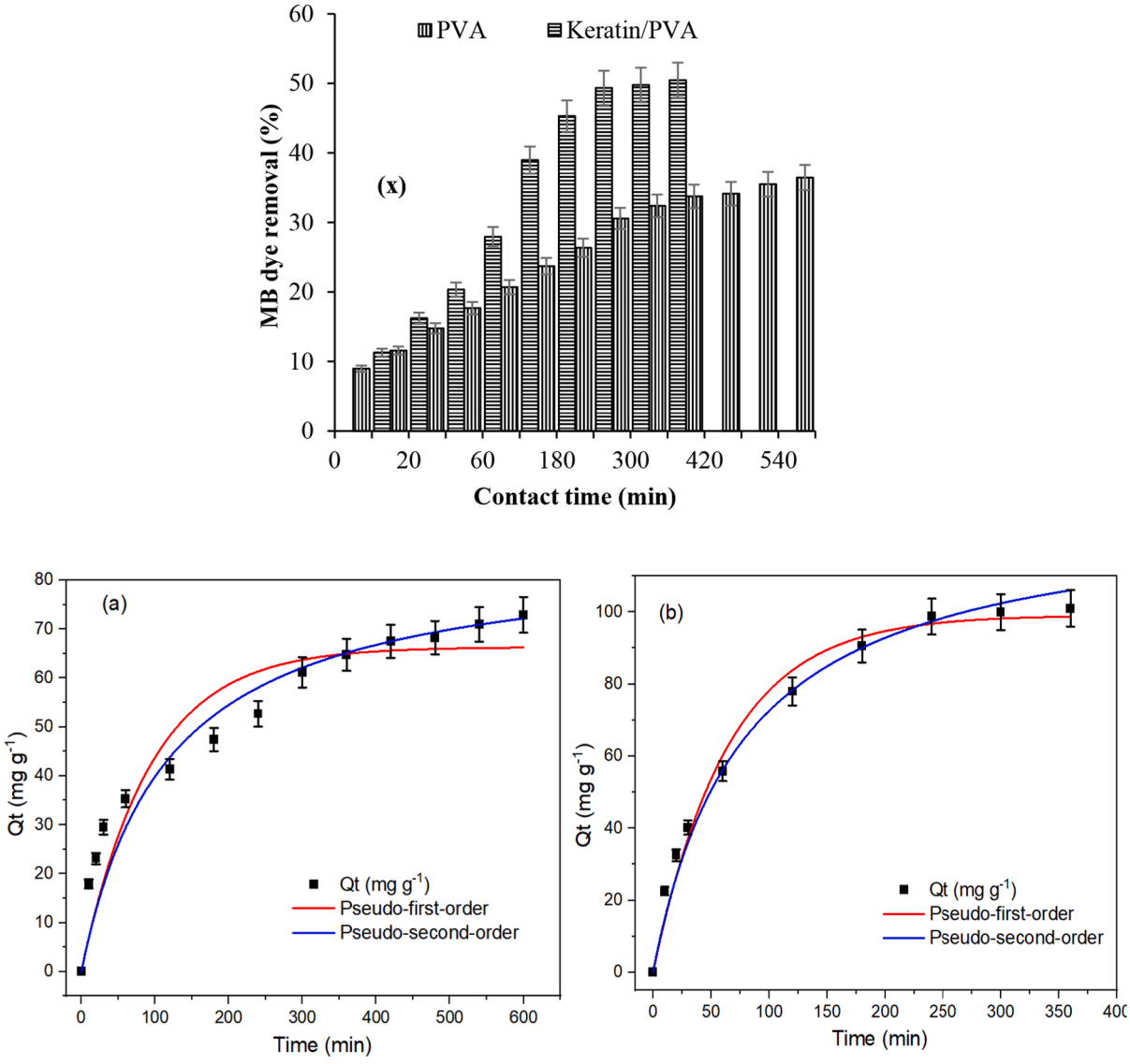

Fig. 5. The dye removal (x) and pseudo-first order and pseudo-second order kinetic models for the MB dye adsorption on PVA (a) and PVA/keratin (b) nanofibrous membranes.

PSO kinetic model can be used to describe the adsorption of MB onto PVA and PVA/keratin nanofibrous membranes. This suggests that the adsorption of MB by the studied nanofibrous membranes is primarily governed by chemisorption and electrostatic attraction between the binding sites of the adsorbent and the MB dye molecules. Previous research showed that the pseudo-second-order kinetic model accurately described the adsorption of MB by other adsorbents [47]. Overall, the present PVA/keratin nanofibrous membrane has a notable capacity for adsorbing MB in a brief duration, implying its suitability for practical use.

3.2.5. Comparison of MB dye adsorption capacities by keratin/PVA nanofibrous membrane with other similar adsorbents

Table 3 shows the MB dye adsorption capacity of several similar adsorbents studied by others. Of them, the nanofibrous membrane adsorbent made from 100 % keratin extracted by sulfitolysis showed a maximum MB binding capacity of 170 mg g^{-1} [31]. The lowest MB dye binding capacity (9.3 mg g^{-1}) was exhibited by sodium alginate/PVA composite nanofibrous membrane [48]. The highest MB dye adsorption capacity (187.0 mg g^{-1}) was exhibited by the sericin/β-cyclodextrin/PVA composite nanofibrous membrane [49], which is considerably lower compared to the keratin/PVA nanofibrous membrane (238.0 mg g^{-1}) reported in this work. The MB dye binding capacity exhibited by the PVA nanofibrous membrane functionalized with poly(methyl vinyl ether-*alt*-maleic anhydride) was 101.0 mg g^{-1} [50]. Nanofiber Membranes The findings shown in the analysis of several adsorbents for MB dye adsorption reveal that the PVA/keratin adsorbent has a considerably superior adsorption capacity compared to the other adsorbents.

3.3. Ionic strength and reusability

Typically, wastewater may include a diverse array of pollutants, including suspended and dissolved solids, acids or alkalis, salts, metal ions, and other elements that pose a risk to human health or the environment. The inclusion of ions in the solution increases the ionic strength, potentially influencing the effectiveness of the adsorption mechanism [52]. To investigate the impact of ionic strength on the adsorption capacity of MB dye by the PVA and PVA/keratin nanofibrous membranes (as shown in Fig. 6a), different amounts of NaCl were introduced into the dye solution in the dye adsorption tests. A correlation was seen between the rise in NaCl content and the corresponding decrease in MB dye adsorption capacity, which is not unusual for the removal of dye by adsorption. The observed phenomenon may be ascribed to the evolutionary process of the electrostatic attraction between the dye molecules and the surfaces of the adsorbents that carry a negative charge, which is affected by the presence of NaCl, particularly at greater concentrations. This can be explained by the fact that the sodium cations (Na^+) present in NaCl compete with the cationic MB dye for the binding sites on the surface of the membrane [53], which consequently decreases dye adsorption. Liu et al. reported a similar observation for the adsorption of MB dye on a cellulose-based bio adsorbent [54]. The generated adsorbent must have a robust reusability and regeneration capacity to effectively compete with commercial dye adsorbents. These properties are often considered to be the primary indicators of an adsorbent's efficacy. Consequently, a set of regeneration cycle experiments was performed using PVA and PVA/keratin nanofibrous membrane, with a maximum of three cycles done under optimum circumstances (Fig. 6b). The experimental results revealed a reduction in adsorption capacity by 22.24 % after three cycles when using PVA alone, but the PVA/keratin nanofibrous membrane exhibited a small reduction (8.95 % only). These findings suggest that the incorporation of keratin into the PVA nanofibrous membrane enhances its reusability compared to the original PVA nanofibrous membrane. The superior performance of the PVA/keratin nanofibrous membrane may be attributed to the presence of anionic carboxyl and Bunte salt groups in keratin as well as the lower nanofiber diameter, which results in a higher surface area. In summary, the efficacy and recyclability of the PVA/keratin nanofibrous membrane indicates its effectiveness as an adsorbent for the purification of actual wastewater.

Table 3
A comparison of the MB adsorption capacity of keratin/PVA nanofibrous membrane with other similar nanofibrous membrane adsorbents cited in published literature.

Adsorbent	pH	Kinetics	Isotherms	q_{max} (mg g^{-1})	Ref.
Keratin	6.0	PSO	Langmuir	170.0	[31]
PVA/graphene oxide	7.0	PSO	Langmuir	110.0	[34]
Sodium alginate/PVA	6.0	PSO	Langmuir	9.3	[49]
Sericin/β-cyclodextrin/PVA	8.0	PSO	Langmuir	187.0	[50]
Poly(methyl vinyl ether-alt-maleic anhydride)/PVA	5.9	PSO	Langmuir	101.0	[51]
Keratin/PVA	7.0	PSO	Langmuir	238.7	This work

3.4. Mechanism of removal of MB dye by keratin/PVA nanofibrous membrane

The mechanism of removal of MB dye by keratin/PVA nanofibrous membrane is shown in Fig. 7. PVA has many hydroxyl and a few methyl ($–CH_3$) groups, but keratin has amino ($–NH_2$), carboxyl (–COOH), and hydroxyl (–OH) groups, as keratin is a poly amino acid composed of 19 amino acids. Wool keratin also has Bunte salt groups ($–S–SO_3Na$) formed by the breakdown of disulfide bonds and oxidation of thiol groups. The amino, carboxyl, and hydroxyl groups of keratin protein form hydrogen bonds with the hydroxyl groups of PVA as shown in Fig. 7, decreasing the water-solubility of keratin. In an aqueous solution, the isoelectric point of wool keratin is 4.5, i.e., below pH 4.5, keratin is cationic but above pH 5, keratin becomes anionic due to the deprotonation of carboxyl and Bunte salt groups of keratin protein [55]. The surface negative charge of keratin increases with an increase in the pH. On the other hand, MB dye has two quaternary ammonium groups making the dye cationic. In acidic conditions, keratin is positively charged and therefore cannot bind positively charged MB dye molecules due to electrostatic repulsion. Some level of dye adsorption was achieved below pH 4.5 due to the hydrophobic-hydrophobic interaction between the hydrophobic methyl groups of PVA and dimethyl groups of MB dye. At pH 7, the keratin protein and PVA surface become negatively charged. This results in an electrostatic attraction between positively charged MB dye and negatively charged keratin and PVA. The membrane-MB dye interaction exhibited maximal attraction at a neutral pH, leading to an enhanced adsorption capacity. The maximum removal of MB dye by the keratin/PVA nanofibrous membrane occurred at pH 7 as cationic quaternary ammonium groups of MB dye form ionic bonds with the anionic carboxyl and Bunte salt groups of wool keratin protein. The electrostatic attraction between the dye and the keratin of the keratin/PVA nanofibrous membrane played a key role in removing the MB dye from its aqueous solution. Therefore, the Keratin/PVA nanofibrous membrane showed high MB dye binding capacity compared to the neat PVA nanofibrous membrane, which only contains weakly anionic hydroxyl groups.

4. Conclusions

Keratin possesses many functional groups, such as carboxyl and Bunte salt groups that render it potentially suitable for the removal of cationic dyes from industrial wastewater. This work demonstrated that fine nanofibrous membrane can be formed from S-sulfonated keratin by electrospinning by using high molecular weight PVA as a carrier, and the developed keratin/PVA nanofibrous adsorbent showed excellent cationic dye removal capacity. The morphological characterization by

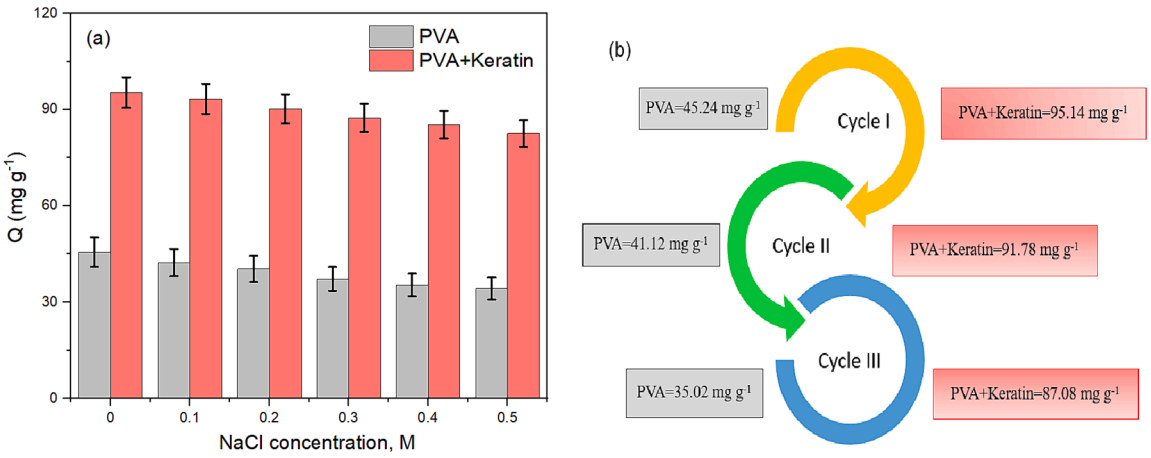

Fig. 6. Effect of ionic strength (a) and reusability (b) for PVA and PVA/keratin nanofibrous membrane.

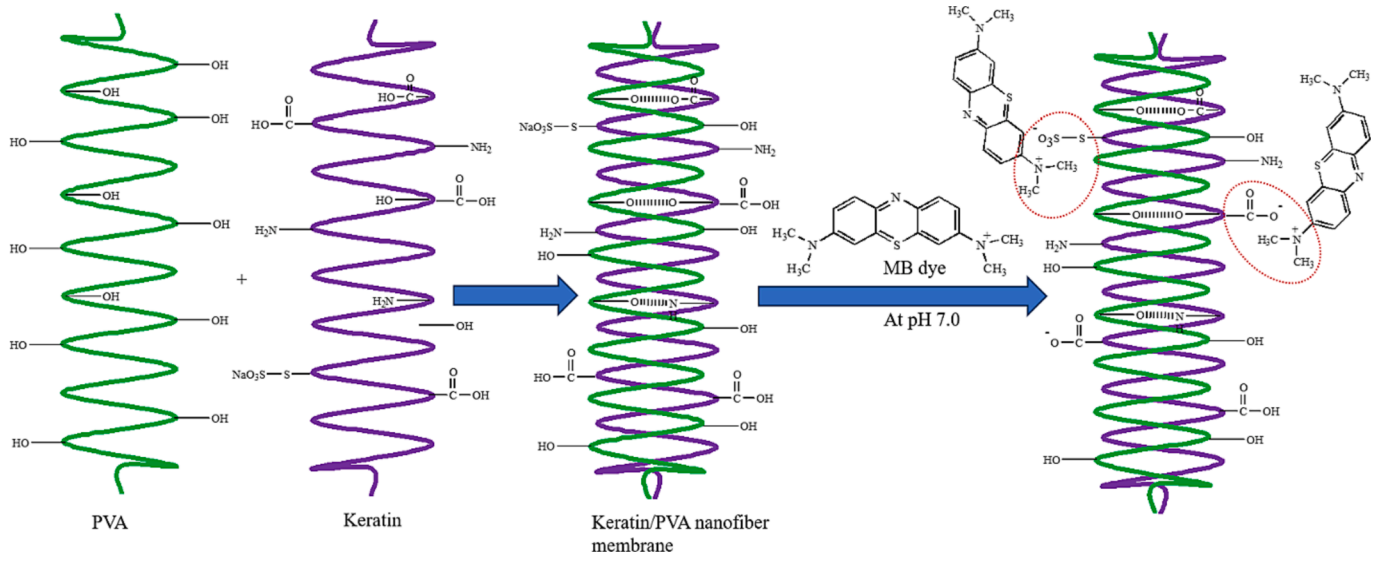

Fig. 7. Mechanism of removal of MB dye by keratin/PVA nanofibrous membrane.

SEM shows that electrospinning produced keratin/PVA nanofiber with a smooth surface and had an exceptionally small diameter (79 nm), compared to the nanofibers produced from neat PVA, which had a larger diameter of 255.0 nm. The batch adsorption studies show that the MB dye adsorption by PVA/keratin nanofibrous membrane adsorbent reached equilibrium in 240 min with 75 % of the MB dye adsorbed within the first 120 min. In contrast, the pure PVA nanofibrous membrane adsorbent needed more than 400 min to reach equilibrium. Furthermore, the kinetics data indicated that the PSO model outperformed the PFO model for MB dye adsorption by keratin/PVA nanofibrous membrane. The analysis of the adsorption isotherms indicates that the PVA/keratin blended nanofibrous membrane exhibited a remarkably high adsorption capacity for MB dye (238.7 mg g^{-1}) at pH 7 at room temperature. The MB dye adsorption capacity achieved by the keratin/PVA nanofibrous membrane was considerably higher than the MB dye adsorption capacity exhibited by the neat PVA nanofibrous membrane (94.9 mg g^{-1}). The MB dye adsorption is better fitted with the Langmuir model than the Freundlich model. In relation to the ionic strength, it was observed that the adsorption capacity of the PVA/keratin composite was negatively affected by an increase in the concentration of ionic strength of the treatment solution. The developed adsorbent showed good recycling and reusability as after 3 three recycling and reuse, only a small loss in dye binding capacity was observed, which is obvious for any adsorbent. The developed keratin/PVA electrospun nanofibrous membrane demonstrated quite a high MB dye-binding capacity with good reusability and minimal effect by other contaminants present in the effluent exhibiting great promise for the removal of cationic dyes from industrial effluent.

CRediT authorship contribution statement

Md. Nahid Pervez: Investigation, Writing – original draft. **Mohammad Mahbubul Hassan:** Conceptualization, Investigation, Writing – review & editing, Project administration, Funding acquisition, Supervision. **Vincenzo Naddeo:** Project administration, Funding acquisition, Supervision.

Declaration of competing interest

The authors declare that they have no known competing financial interests or personal relationships that could have appeared to influence the work reported in this paper.

Data availability

Data will be made available on request.

Acknowledgments

We would like to express our sincere gratitude for the financial support received from the Ministry of Business Innovation and Employment (MBIE) of the New Zealand Government through Grant # C10X0824, and the Sanitary Environmental Engineering Division (SEED) and grants (FARB projects) from the University of Salerno, Italy.

Appendix A. Supplementary data

Supplementary data to this article can be found online at https://doi.org/10.1016/j.seppur.2023.125903.

References

[1] M.M. Hassan, C.M. Carr, Biomass-derived porous carbonaceous materials and their composites as adsorbents for cationic and anionic dyes: a review, Chemosphere 265 (2021), 129087.
[2] M.M. Hassan, C.M. Carr, A critical review on recent advancements of the removal of reactive dyes from dyehouse effluent by ion-exchange adsorbents, Chemosphere 209 (2018) 201–219.
[3] G. Bayramoglu, B. Altintas, M.Y. Arica, Adsorption kinetics and thermodynamic parameters of cationic dyes from aqueous solutions by using a new strong cation-exchange resin, Chem. Eng. J. 152 (2009) 339–346.
[4] Z.-M. Xiong, J.Y. Choi, K. Wang, H. Zhang, Z. Tariq, D. Wu, E. Ko, C. Ladana, H. Sesaki, K. Cao, Methylene blue alleviates nuclear and mitochondrial abnormalities in progeria, Aging Cell 15 (2016) 279–290.
[5] M.N. Pervez, M. Balakrishnan, S.W. Hasan, K.-H. Choo, Y. Zhao, Y. Cai, T. Zarra, V. Belgiorno, V. Naddeo, A critical review on nanomaterials membrane bioreactor (NMs-MBR) for wastewater treatment, npj Clean, Water 3 (2020) 43.
[6] M.M. Hassan, C.J. Hawkyard, Decolorization of dyes and dyehouse effluent in a bubble-column reactor by heterogeneous catalytic ozonation, J. Chem. Technol. Biotechnol. 81 (2006) 201–207.
[7] M.M. Hassan, C.J. Hawkyard, P.A. Barratt, Decolorization of dyes and dyehouse effluent in a bubble-column reactor by ozonation in the presence of H_2O_2, $KMnO_4$ or Ferral, J. Chem. Technol. Biotechnol. 81 (2006) 158–166.
[8] M.M. Hassan, C.J. Hawkyard, Decolorization of aqueous dyes by sequential oxidation treatment with ozone and Fenton's reagent, J. Chem. Technol. Biotechnol. 77 (2002) 834–841.
[9] M.N. Pervez, G.K. Stylios, Y. Liang, F. Ouyang, Y. Cai, Low-temperature synthesis of novel polyvinylalcohol (PVA) nanofibrous membranes for catalytic dye degradation, J. Cleaner Prod. 262 (2020), 121301.
[10] J. Yu, S. Tian, A. Yao, H. Hu, J. Lan, L. Yang, X. Du, S. Lin, Compressible polydopamine modified pomelo peel powder/poly(ethyleneimine)/κ-carrageenan aerogel with pH-tunable charge for selective removal of anionic and cationic dyes, Carbohyd. Polym. 323 (2024), 121377.
[11] L. Yang, J. Shang, B. Dou, J. Lan, C. Zhang, R. Zou, H. Xiao, S. Lin, CO_2-responsive functional cotton fibers decorated with Ag nanoparticles for "smart" selective and enhanced dye adsorption, J. Hazard. Mater. 429 (2022), 128327.
[12] Y.-J. Won, J. Lee, D.-C. Choi, H.R. Chae, I. Kim, C.-H. Lee, I.-C. Kim, Preparation and Application of Patterned Membranes for Wastewater Treatment, Environ. Sci. Technol. 46 (2012) 11021–11027.
[13] H. Chen, M. Huang, Y. Liu, L. Meng, M. Ma, Functionalized electrospun nano membranes for water treatment: a review, Sci. Total Environ. 739 (2020), 139944.
[14] J. Xue, T. Wu, Y. Dai, Y. Xia, Electrospinning and electrospun nanofibers: methods, materials, and applications, Chem. Rev. 119 (2019) 5298–5415.
[15] E.I. El-Aswar, H. Ramadan, H. Elkik, A.G. Taha, A comprehensive review on preparation, functionalization and recent applications of nano membranes in wastewater treatment, J. Environ. Manag. 301 (2022), 113908.
[16] M.E. Talukder, M.N. Pervez, W. Jianming, Z. Gao, G.K. Stylios, M.M. Hassan, H. Song, V. Naddeo, Chitosan-functionalized sodium alginate-based electrospun nano membrane for As (III) removal from aqueous solution, J. Environ. Chem. Eng. 9 (2021), 106693.
[17] M.E. Talukder, M.N. Pervez, W. Jianming, G.K. Stylios, M.M. Hassan, H. Song, V. Naddeo, A. Figoli, Ag nanoparticles immobilized sulfonated polyethersulfone/polyethersulfone electrospun nano membrane for the removal of heavy metals, Sci. Rep. 12 (2022) 5814.
[18] F. Ahmadijokani, H. Molavi, A. Bahi, S. Wuttke, M. Kamkar, O.J. Rojas, F. Ko, M. Arjmand, Electrospun nanofibers of chitosan/polyvinyl alcohol/UiO-66/nanodiamond: versatile adsorbents for wastewater remediation and organic dye removal, Chem. Eng. J. 457 (2023), 141176.
[19] A.S.M. Ali, M.R, El-Aassar, F.S, Hashem, N.A, Moussa, Surface modified of cellulose acetate electrospun nanofibers by polyaniline/β-cyclodextrin composite for removal of cationic dye from aqueous medium, Polym. 20 (2019) 2057–2069.
[20] R.A. Hakro, M. Mehdi, R.F. Qureshi, R.B. Mahar, M. Khatri, F. Ahmed, Z. Khatri, I. S. Kim, Efficient removal of reactive blue-19 dye by co-electrospun nanofibers, Mater. Res. Exp. 8 (2021), 055502.
[21] S. Aziz, M. Sabzi, A. Fattahi, E. Arkan, Electrospun silk fibroin/PAN double-layer nanofibrous membranes containing polyaniline/TiO_2 nanoparticles for anionic dye removal, J. Polym. Res. 24 (2017) 140.
[22] P. Hill, H. Brantley, M. Van Dyke, Some properties of keratin biomaterials: kerateines, Biomaterials 31 (2010) 585–593.
[23] M.M. Hassan, C.M. Carr, A review of the sustainable methods in imparting shrink resistance to wool fabrics, J. Adv. Res. 18 (2019) 39–60.
[24] M.T. Abdu, K.A. Abuhasel, M. Alquraish, S. Nagy, S. Khodir, A.A. Ali, Selected natural s and their electrospinning, J. Polym. Res. 30 (2023) 340.
[25] A.M. Abd El-aziz, A. El-Maghraby, N.A. Taha, Comparison between polyvinyl alcohol (PVA) nano and polyvinyl alcohol (PVA) nano/hydroxyapatite (HA) for removal of Zn2+ ions from wastewater, Arabian J. Chem. 10 (2017) 1052–1060.
[26] H. Yin, J. Zhao, Y. Li, L. Huang, H. Zhang, L. Chen, A novel Pd decorated polydopamine-SiO2/PVA electrospun nano membrane for highly efficient degradation of organic dyes and removal of organic chemicals and oils, J. Cleaner Prod. 275 (2020), 122937.
[27] A.D.S. Montallana, B.-Z. Lai, J.P. Chu, M.R. Vasquez, Enhancement of photodegradation efficiency of PVA/TiO_2 nano composites via plasma treatment, Mater. Today Commun. 24 (2020), 101183.
[28] M.R. Karim, M.O. Aijaz, N.H. Alharth, H.F. Alharbi, F.S. Al-Mubaddel, M.R. Awual, Composite nanofibers membranes of poly(vinyl alcohol)/chitosan for selective lead (II) and cadmium(II) ions removal from wastewater, Ecotoxicol. Environ. Safety 169 (2019) 479–486.
[29] M. Ranjbar-Mohammadi, P. Shakoori, Z. Arab-Bafrani, Design and characterization of keratin/PVA-PLA nanofibers containing hybrids of nanofibrillated chitosan/ZnO nanoparticles, Int. J. Biologic. Macromol. 187 (2021) 554–565.
[30] S. Jung, B. Pant, M. Climans, G. Curtis Shaw, E.-J. Lee, N. Kim, M. Park, Transformation of electrospun Keratin/PVA nano membranes into multilayered 3D Scaffolds: physiochemical studies and corneal implant applications, Int. J. Pharmaceut. 610 (2021), 121228.
[31] A. Aluigi, F. Rombaldoni, C. Tonetti, L. Jannoke, Study of Methylene Blue adsorption on keratin nanofibrous membranes, J. Hazard. Mater. 268 (2014) 156–165.
[32] E. Serag, A.M. Abd El-Aziz, A. El-Maghrabi, N.A. Taha, Electrospun non-wovens potential wound dressing material based on polyacrylonitrile/chicken feathers keratin nanofiber, Sci. Rep. 12 (2022) 15460.
[33] C.S. Ki, E.H. Gang, I.C. Um, Y.H. Park, Nanofibrous membrane of wool keratose/silk fibroin blend for heavy metal ion adsorption, J. Membr. Sci. 302 (2007) 20–26.
[34] Y. He, H. Tian, A. Xiang, S. Ma, D. Yin, A. Varada Rajulu, Fabrication of PVA/GO nano films by electrospinning: application for the adsorption of Cu2+ and organic dyes, J. Polym. Environ. 30 (2022) 2964–2975.
[35] S.H. Tan, R. Inai, M. Kotaki, S. Ramakrishna, Systematic parameter study for ultra-fine fabrication via electrospinning process, Polymer 46 (2005) 6128–6134.
[36] J. Wang, L. Ye, Structure and properties of polyvinyl alcohol/polyurethane blends, Composites b: Eng. 69 (2015) 389–396.
[37] K. Katoh, M. Shibayama, T. Tanabe, K. Yamauchi, Preparation and properties of keratin–poly(vinyl alcohol) blend, J. Appl. Polym. Sci. 91 (2004) 756–762.
[38] M. He, B. Zhang, Y. Dou, G. Yin, Y. Cui, X. Chen, Fabrication and characterization of electrospun feather keratin/poly(vinyl alcohol) composite nanofibers, RSC Adv. 7 (2017) 9854–9861.
[39] M.M. Hassan, Wool fabrics coated with an anionic bunte salt-terminated polyether: physicomechanical properties, stain resistance, and dyeability, ACS Omega 3 (2018) 17656–17667.
[40] K. László, A. Szűcs, Surface characterization of polyethyleneterephthalate (PET) based activated carbon and the effect of pH on its adsorption capacity from aqueous phenol and 2,3,4-trichlorophenol solutions, Carbon 39 (2001) 1945–1953.
[41] T.T. Nguyen, T.K. Phung, X.-T. Bui, V.-D. Doan, T.V. Tran, D.V. Nguyen, K.T. Lim, T.D. Nguyen, Removal of cationic dye using polyvinyl alcohol membrane functionalized by D-glucose and agar, J. Water Process Eng. 40 (2021), 101982.
[42] C. Bouyahia, M. Rahmani, M. Bensemlali, S. El Hajjaji, M. Slaoui, I. Bencheikh, K. Azoylay, N. Labjar, Influence of extraction techniques on the adsorption capacity of methylene blue on sawdust: optimization by full factorial design, Mater. Sci. Energ. Technol. 6 (2023) 114–123.
[43] A.S. Ibupoto, U.A. Qureshi, F. Ahmed, Z. Khatri, M. Khatri, M. Maqsood, R.Z. Brohi, I.S. Kim, Reusable carbon nanofibers for efficient removal of methylene blue from aqueous solution, Chem. Eng. Res. Design 136 (2018) 744–752.
[44] V.O. Shikuku, T. Mishra, Adsorption isotherm modeling for methylene blue removal onto magnetic kaolinite clay: a comparison of two-parameter isotherms, Appl. Water Sci. 11 (2021) 103.
[45] M.N. Pervez, Y. Wei, P. Sun, G. Qu, V. Naddeo, Y. Zhao, α-FeOOH quantum dots impregnated graphene oxide hybrids enhanced arsenic adsorption: the mediation role of environmental organic ligands, Sci. Total Environ. 781 (2021), 146726.
[46] M.N. Morshed, M.N. Pervez, N. Behary, N. Bouazizi, J. Guan, V.A. Nierstrasz, Statistical modeling and optimization of heterogeneous Fenton-like removal of organic pollutant using fibrous catalysts: a full factorial design, Sci. Rep. 10 (2020) 16133.
[47] M. Luo, M. Wang, H. Pang, R. Zhang, J. Huang, K. Liang, P. Chen, P.-P. Sun, B. Kong, Super-assembled highly compressible and flexible cellulose aerogels for methylene blue removal from water, Chinese Chem. Lett. 32 (2021) 2091–2096.
[48] M. Maruthapandi, V.B. Kumar, J.H.T. Luong, A. Gedanken, Kinetics, isotherm, and thermodynamic studies of methylene blue adsorption on polyaniline and polypyrrole macro-nanoparticles synthesized by C-dot-initiated polymerization, ACS Omega 3 (2018) 7196–7203.
[49] X. Jiang, C. Sang, J. Wang, J. Guo, Preparation of sodium alginate/polyvinyl alcohol composite nano membranes for adsorption of dyes, Text. Res. J. 92 (2022) 3154–3163.
[50] R. Zhao, Y. Wang, X. Li, B. Sun, Z. Jiang, C. Wang, Water-insoluble sericin/β-cyclodextrin/PVA composite electrospun nanofibers as effective adsorbents towards methylene blue, Colloid. Surf. B: Biointerf. 136 (2015) 375–382.

[51] M. Xiao, J. Chery, M.W. Frey, Functionalization of electrospun Poly(vinyl alcohol) (PVA) nano membranes for selective chemical capture, ACS Appl. Nano Mater. 1 (2018) 722–729.
[52] D. Alipour, A.R. Keshtkar, M.A. Moosavian, Adsorption of thorium(IV) from simulated radioactive solutions using a novel electrospun PVA/TiO2/ZnO nano adsorbent functionalized with mercapto groups: study in single and multi-component systems, Appl. Surf. Sci. 366 (2016) 19–29.
[53] D. Nie, P. Wang, C. Zang, G. Zhang, S. Li, R. Liu, Y. Zhang, Y. Luo, W. Zhang, J. Dai, Preparation of ZnO-incorporated porous carbon nanofibers and adsorption performance investigation on methylene blue, ACS Omega 7 (2022) 2198–2204.
[54] L. Liu, Z.Y. Gao, X.P. Su, X. Chen, L. Jiang, J.M. Yao, Adsorption removal of dyes from single and binary solutions using a cellulose-based bioadsorbent, ACS Sust. Chem. Eng. 3 (2015) 432–442.
[55] E.-M. Nuutinen, J.J. Valle-Delgado, M. Kellock, M. Farooq, M. Österberg, Affinity of keratin peptides for cellulose and lignin: a fundamental study toward advanced bio-based materials, Langmuir 38 (2022) 9917–9927.